





Analysis of adiabatic processes in multilevel N-pod quantum systems from the perspective of Riemannian geometry

Arturs Cinins^{1,a}, Milan S. Dimitrijević^{2,3} , Vladimir A. Srećković⁴, Kaspars Miculis¹, and Nikolai N. Bezuglov⁵ 

¹ Institute of Atomic Physics and Spectroscopy, University of Latvia, Jelgavas Str. 3, Riga 1004, Latvia

² Astronomical Observatory, Volgina 7, Belgrade 11060, Serbia

³ LERMA, Observatoire de Paris, Université PSL, CNRS, Sorbonne Université, 92190 Meudon, France

⁴ Institute of Physics Belgrade, University of Belgrade, Belgrade 11080, Serbia

⁵ Saint Petersburg State University, 7/9 Universitetskaya nab., St. Petersburg, Russia 199034

Received 30 December 2022 / Accepted 12 April 2023 / Published online 30 May 2023

© The Author(s), under exclusive licence to EDP Sciences, SIF and Springer-Verlag GmbH Germany, part of Springer Nature 2023

Abstract. The analysis of problems related to nonlocalized population transfer between quantum levels requires nontraditional mathematical approaches. Here we study the processes of irremovable nonadiabatic transitions in a $(N - 1)$ -dimensional system of completely degenerate so-called dark states, taking as a base model multilevel N-pod systems. It is shown that quantum dynamics of the dark states due to the operator of nonadiabatic coupling can be described in terms of the Riemannian parallel transport of their geometric counterparts in the space of control parameters. The results of mathematical modeling of nonadiabatic effects, presented in the paper for the case of four-level systems interacting with three laser fields (tripod systems), demonstrate full agreement between the quantum and geometric approaches. These results are of interest for experimental and laboratory plasma research and atomic and laser physics.

1 Introduction

Adiabatic processes play an important role in natural phenomena. In physical kinetics, for instance, they largely determine the rates of reactions involving various elementary and compound particles [1], while in quantum optics the adiabatic control of atomic ensembles driven by laser fields results in a large number of practically important interference effects [2, 3] which, in particular, make it possible to implement some basic quantum gates [4]. Population transfer between energy states in quantum systems with slowly (adiabatically) changing parameters (i.e., internuclear distances R , intensities I of external control fields, etc.) is traditionally described within the formalism of the adiabatic [5] or in the so-called quantum optics dressed [6] states. In this formalism, the quantum dynamics of a system is determined by the nonadiabatic coupling operator and critically depends on the structural features of the adiabatic energy diagrams.

T.I.: Physics of Ionized Gases and Spectroscopy of Isolated Complex Systems: Fundamentals and Applications.

Guest editors: Bratislav Obradović, Jovan Cvetić, Dragana Ilić, Vladimir Srećković and Sylwia Ptasinska.

^a e-mail: arturs.cinins@lu.lv (corresponding author)

The simplest but at the same time practically important case corresponds to the localization of nonadiabatic transitions in the vicinity of the quasi-intersection points R_0 (Landau–Zener points) of two energy curves (see Fig. 1). A theory, developed for calculating the corresponding probabilities rates by Landau and Zener [1, 7] with its further improvement by Dykhne, Davis and Pechukas [8, 9], is widely used in the scientific literature for calculating collisional and radiation elementary processes in the approximation of two-level quantum systems (see Fig. 1a, b). The adiabatic criterion resulting in low collision rate constants is controlled by large values of the adiabatic parameter (also called Massey parameter) ξ [1]:

$$\xi = \frac{\Delta U}{\hbar} \frac{\delta R}{v} = \frac{\Delta U}{\hbar} \tau \gg 1, \quad (1)$$

where $\Delta U = \Delta U(R_0)$ is the adiabatic splitting of the energy curves at the Landau–Zener point R_0 , v is the internuclear velocity at that point, while τ corresponds to the characteristic time of the atomic transition under study. Pay attention that the temporal dynamics of any two-level system can be effectively described in geometric terms associated with the parametrization of the corresponding density matrices [10] as a polarization vector on the so-called unit two-dimensional Bloch sphere [10, 11].

An increase in the dimension of quantum systems leads to significantly more complicated analytical and numerical description of their dynamic features. It particularly concerns the analysis of mixing between permanently degenerate adiabatic states (see Fig. 1c) that requires studying the entire time interval of the process under consideration, thus significantly complicating the theoretical methods used.

In this article, implementing the situation presented in Fig. 1c with an N-pod system [12] and focusing on a tripod excitation scheme (see Fig. 2a), we show that adiabatic evolution of such systems for a given sequence of laser excitation pulses can be interpreted as Riemannian parallel transport [13, 14] of a tangent state vector along the surface of an (N - 1)-dimensional Bloch sphere. This approach presents a convenient tool for the analysis of adiabatic quantum processes involving high-dimensional systems.

2 Structural features of N-pod systems

We are studying the following excitation scheme, in the literature associated with N-pod atomic configuration [12]: A single excited quantum state $|2\rangle$ is coupled with N components $|j\rangle$ ($j = 1, 3, 4, \dots, N + 1$) of the ground state via N laser electrical fields $\mathbf{E}_j(t) \cos(\omega_j t)$. The

Pump (P) and Stokes (S) lasers usually [4] drive the level population transfer, while the other $N - 2$ lasers ($Q, \dots, N + 1$) play an auxiliary or control role, depending on the task to be performed [12]. As will be shown below, all N-pod systems, regardless of their dimension, share the structure of adiabatic states, enabling investigation of their properties from a unified position. In this section, on the basis of differential geometry methods we offer a universal approach to describing the nonadiabatic quantum dynamics of such systems.

For a given temporal sequence of laser pulses, accurate analysis of our system requires finding the evolution of the state wave vector $\psi(t)$ from the Schrödinger equation. In the framework of rotating wave approximation (RWA) [6, 11], the latter reads:

$$i\hbar \frac{d}{dt} \psi = \hat{H}_{RW} \psi; \quad \hat{H}_{RW} = \varepsilon |2\rangle \langle 2| + \hat{V} + \hat{V}^\dagger; \quad (2)$$

$$\hat{V}(t) = \frac{\hbar}{2} \sum_{j=1,3,\dots,N+1} \Omega_j(t) |j\rangle \langle 2|;$$

$$\Omega_j(t) = (2/\hbar) \langle j | \hat{V}(t) | 2 \rangle \quad (3)$$

The Rabi frequencies $\Omega_j(t)$ describe the lasers/atom interaction and depend on the fields amplitudes $\mathbf{E}_j(t)$ and dipole matrix elements \mathbf{d}_{2j} of the corresponding optical transitions: $\Omega_j(t) = \mathbf{E}_j(t) \cdot \mathbf{d}_{2j}$ [6]. Here

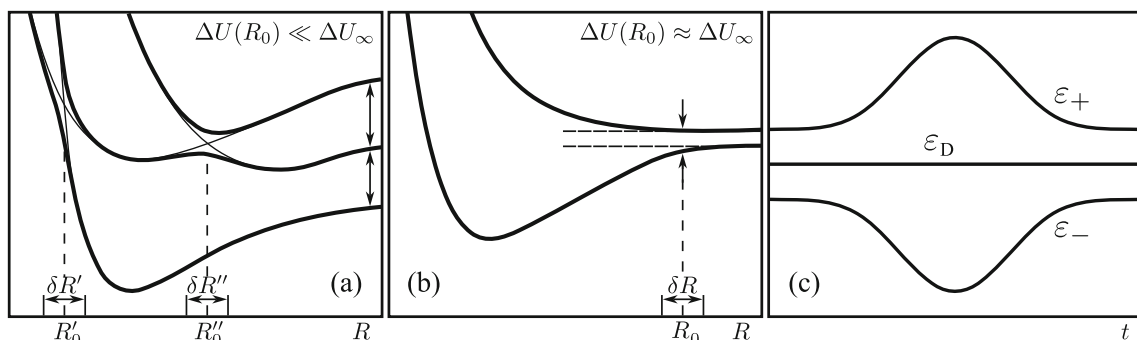


Fig. 1 Energy level diagrams for a few typical situations with localized (frames **a**, **b**) and delocalized (frame **c**) atomic transitions. In the case of frames (**a**, **b**), transitions are localized in the neighborhood δR of quasi-crossing points R_0 , while frame (**b**) corresponds to irremovable and permanent nonadiabatic transitions between degenerate sublevels with energy ε_D

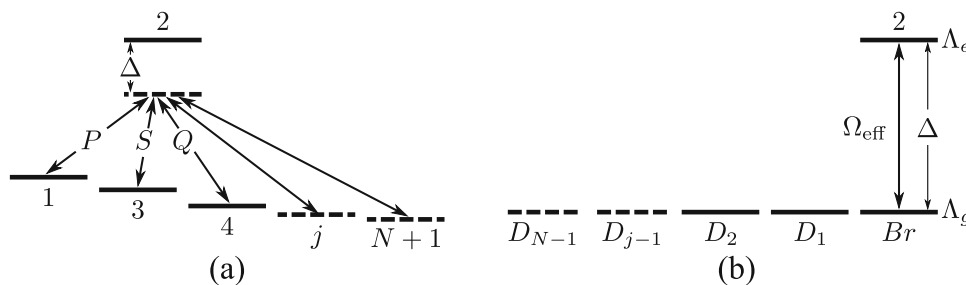


Fig. 2 Linkage diagram (**a**) and diabatic states (**b**) in tripod (N-pod) systems. **a** Three lasers P, S, Q couple the sublevels $|1\rangle, |3\rangle, |4\rangle$ of the ground subspace Λ_g to the excited state $|2\rangle$. The parameter Δ denotes the single-photon detuning. **b** Morris-Shore reduction of the excitation scheme (**a**) to a set of decoupled (dark) adiabatic states $|D\rangle_{1,2(\dots,N-1)}$ and a single coupled (bright) diabatic state $|Br\rangle$. Dashed lines represent the additional ground sublevels $|j\rangle, j > 4$ for N-pod systems with $N > 3$

we assume all the lasers have the same single-photon detuning Δ that determines the following structure of the first diagonal atomic operator in the Hamiltonian \widehat{H}_{RW} of the N-pod system (2): (i) all the diabatic (or “bare” in the terminology of quantum optics) ground sublevels $|j\rangle$ are mutually degenerate, and with appropriate choice of the RWA reference energy level, their energies are equal to zero; (ii) accordingly, the energy ε of the upper bare state $|2\rangle$ has to be equal to the single-photon detuning, $\varepsilon = \hbar\Delta$. The second and third interaction operators $\widehat{V}(t), \widehat{V}(t)^\dagger$ (2) in the Hamiltonian \widehat{H}_{RW} are responsible for mixing the excited and ground atomic levels due to the laser fields with slowly varying Rabi frequencies $\Omega_j(t)$ (3). Importantly, the operator $\widehat{V}(t)$ maps the excited state $|2\rangle$ onto the ground sublevels $|j\rangle$ and vice versa for its conjugated operator $\widehat{V}(t)^\dagger$. We further assume as well that all the laser Rabi frequencies are real-valued.

2.1 Adiabatic states in a system of two degenerate states

An important theoretical tool in the study of adiabatic processes is a formalism operating with a complete set of adiabatic states (or laser dressed states [4]) ψ_m . These states are the full set of eigenfunctions $\widehat{H}_{RW}(t)\psi_m(t) = \varepsilon_m(t) \cdot \psi_m(t)$, ($m = 1, \dots, N + 1$) of the Hamiltonian \widehat{H}_{RW} (2). Their corresponding eigenvalues spectrum ε_k determines the structure of the energy level diagram. A remarkable property of the N-pod configuration is the capability to partition the $(N + 1)$ adiabatic states into two universal submanifolds Λ_{Br} and Λ_D . The first submanifold Λ_{Br} is two-dimensional and consists of two orthogonal wave functions $|e, Br\rangle, |g, Br\rangle$ arising from interaction with the control laser fields and is therefore termed “bright.” The second $(N - 1)$ -dimensional submanifold Λ_D is comprised of $(N - 1)$ wave functions $|D\rangle_k$ in the ground state, which are decoupled from the external interaction (see Fig. 2b) and are called “dark” in the literature on quantum optics [4, 15].

In the case of a laser-coupled two-level system with degenerate sublevels (N_g sublevels in the ground manifold Λ_g and N_e sublevels ($N_e < N_g$) in the excited manifold Λ_e), Morris and Shore in their work [16] have suggested a universal method for finding all the adiabatic (dressed) states (for use case in a realistic multistate quantum system, see [17]). According to the Morris–Shore method, the eigenfunctions

$$\widehat{V}^\dagger \widehat{V} |e, Br\rangle_i = \Gamma_i^2 \cdot |e, Br\rangle_i; \Gamma_i^2 = \langle e, Br | \widehat{V}^\dagger \widehat{V} |e, Br\rangle_i \tag{4}$$

of the positive Hermitian operator $\widehat{V}(t)^\dagger \widehat{V}(t)$ provide in the subspace Λ_e a normalized set of orthogonal N_e “bright” (Br) diabatic (also “bare” [4]) wave vectors

$|e, Br\rangle_i$ ($i = 1, \dots, N_e$). Their N_e images

$$|g, Br\rangle_i = \frac{1}{\Gamma_i} \widehat{V} |e, Br\rangle_i \tag{5}$$

form in the ground subspace Λ_g the orthogonal subset of “bright” wave vectors $|g, Br\rangle_i$, each coupled to its pre-image $|e, Br\rangle_i$ by the interaction operator \widehat{V}^\dagger (as shown in Fig. 2b where $N_e = 1$ and $|e, Br\rangle_1 = |2\rangle$). Noteworthy, the eigenvalues Γ_i^2 satisfy the conventional relation (4) [5, 7].

Any vector $|g, D\rangle$ of the ground subspace that is orthogonal to all bright vectors, i.e.,

$$\langle g, D | |g, Br\rangle_i = \langle g, D | \widehat{V} |e, Br\rangle_i / \Gamma_i = 0, \tag{6}$$

turns out, as seen from Eq. (5), to be decoupled from the excited state and therefore belongs to the dark linear manifold Λ_D of dimension $N_g - N_e$. The union of all the orthogonal vectors $|g, Br\rangle_i$ with the full set $|g, D\rangle_k$ ($k = 1, \dots, N_g - N_e$) of basis vectors from the manifold Λ_D produces in the ground subspace Λ_g the so-called Morris–Shore (MS) basis. The latter, thus, consists of a set of coupled “bright” states (BS) and entirely decoupled “dark” states (DS).

2.2 The Morris–Shore basis for N-pod systems

The N-pod configuration depicted in Fig. 2 corresponds to a nondegenerate excited state ($N_e = 1$) with one BS $|e, Br\rangle_1 \equiv |2\rangle$. The bright basis in the ground subspace, therefore, contains a single vector $|g, Br\rangle_{i=1} \equiv |Br\rangle$. The expressions (4), (5) provide an explicit analytical representation of that normalized BS $|Br\rangle$:

$$|Br\rangle = \frac{1}{2} \sum_{j \neq 2} \Omega_j |j\rangle / \Gamma; \quad \Gamma = \frac{1}{2} \sqrt{\sum_{j \neq 2} \Omega_j^2} \tag{7}$$

in the initial basis of the ground components $|j\rangle$. Here the interaction operator \widehat{V} (3) is defined via Rabi frequencies of the applied lasers. Note that a straightforward calculation yields

$$\langle 2 | \widehat{H}_{RW} |Br\rangle \equiv \frac{1}{2} \Omega_{\text{eff}} = \frac{1}{\hbar} \langle 2 | \widehat{V} |Br\rangle = \Gamma, \tag{8}$$

i.e., the BS $|Br\rangle$ is strongly coupled to the excited state, with the linkage parameter Ω_{eff} playing the role of the effective Rabi frequency (see Fig. 2b).

A condition (6) that some wave vector

$$|D\rangle = \sum_{j \neq 2} C_j^{(D)} |j\rangle \tag{9}$$

belongs to the dark manifold Λ_D implies orthogonality between the vectors $|D\rangle$ (8) and $|Br\rangle$ (7), or

$$\langle Br|\hat{V}|D\rangle = \frac{1}{2\Gamma} \sum_{j \neq 2} \Omega_j C_j^{(D)} = 0. \tag{10}$$

Noteworthy, upon altering the Rabi frequencies $\Omega_j(t)$, both the BS (7) and the dark manifold Λ_D become time-dependent. The N-pod Hamiltonian \hat{H}_{RW} (2), however, acts in the subspace of dark states as a zero operator $\hat{H}_{RW}|D\rangle = 0$, i.e., all $|D\rangle$ are mutually degenerate adiabatic states with zero energy $\varepsilon_D \equiv 0$, regardless of the laser coupling strengths (see Fig. 2b). On the other hand, the relation (8) determines \hat{H}_{RW} as a two-dimensional operator in the manifold Λ_{Br} of bright vectors. Diagonalization of \hat{H} in Λ_{Br} results in the formation of two adiabatic (dressed) states $|\pm\rangle$ as superpositions of vectors $|Br\rangle$ and $|2\rangle$ with repulsive adiabatic energies [4,17]

$$\varepsilon_{\pm}(t) = \frac{\hbar}{2}\Delta \pm \frac{\hbar}{2}\sqrt{\Delta^2 + \Omega_{\text{eff}}(t)^2}, \tag{11}$$

schematically shown in Fig. 1c.

3 Nonadiabatic transitions as Riemannian parallel transport

Since the dark manifold is energetically degenerate, the nonadiabatic coupling operator causes permanent transitions between dark states. The efficiency of nonadiabatic mixing does not depend on the timescales of the atomic system evolution [4], and as noted in the physical literature [18], the most relevant tool for describing nonadiabatic quantum processes in the subspace of dark states is the theory of gauge (or Yang–Mills) fields [19]. On the other hand, there is an interpretation of the Yang–Mills field as a curvature in the so-called charge space, which for N-pod systems corresponds to the dark manifold (see paragraph 2 of chapter 1 in handbook [19]). Deriving from this interpretation, we provide an approach for solving problems of nonadiabatic dynamics in terms of differential and Riemannian geometries [13,14]; namely, we interpret the effect of nonadiabatic coupling as a result of the Riemannian parallel transport of dark manifold vectors.

3.1 Geometric analogs of the Morris–Shore basis

Assuming all the Rabi frequencies are real, it is possible to associate the set of Ω_j that define the bright wave vector $|Br\rangle$ (7) with components of a Rabi vector $\mathbf{R} = (\Omega_P, \Omega_S, \Omega_Q, \Omega_5, \dots, \Omega_{N+1})$ in Euclidean parameter space \mathfrak{R}_N :

$$\mathbf{R} = \Omega_P \mathbf{e}_P + \Omega_S \mathbf{e}_S + \Omega_Q \mathbf{e}_Q$$

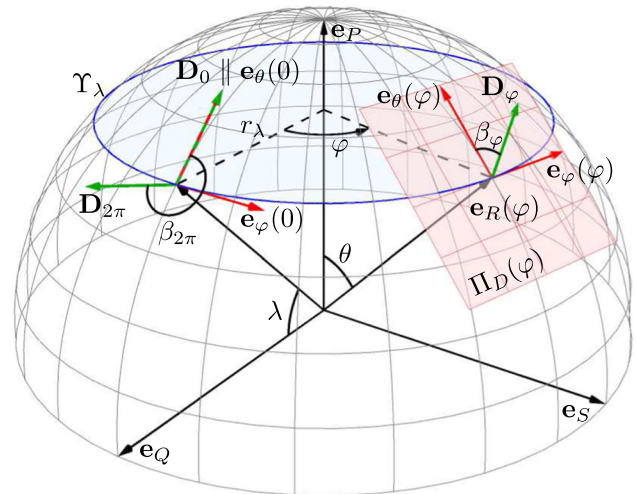


Fig. 3 Geometric representations of bright and dark quantum states of the tripod system ($N = 1$) as a unit vector \mathbf{e}_r (a counterpart of $|Br\rangle$) and a tangent d-vector \mathbf{D}_φ (a geometrical counterpart of $|D\rangle$) on the Bloch sphere. For convenience, all normalized to unity tangent vectors are shown reduced in length, and the bottom half of the sphere is not shown

$$+ \sum_{j=5, \dots, N+1} \Omega_j \mathbf{e}_j; \quad \mathbf{e}_r = \frac{\mathbf{R}}{|\mathbf{R}|}. \tag{12}$$

As the Rabi frequencies change, the Rabi vector $\mathbf{R}(t)$ (12) moves along some curve \mathfrak{S}_R in the above parameter space \mathfrak{R}_N . At the same time, the corresponding counterpart $\mathbf{e}_r(t)$ (12) of the unit bright vector $|Br\rangle$ (7) draws a Rabi path $\mathfrak{S}_1 = \hat{\Xi}_{R \rightarrow 1} \mathfrak{S}_R$, which is the radial projection of the curve \mathfrak{S}_R , on the $(N - 1)$ -dimensional unit sphere (a generalization of the Bloch sphere) embedded in the parameter space \mathfrak{R}_N (see Fig. 3).

We can also associate the probability amplitudes C_j of a dark state vector $|D\rangle$ (9) with the components of an Euclidean vector $\mathbf{D} \sim (C_P, C_S, C_Q, \dots, C_N)$ in \mathfrak{R}_N ,

$$\mathbf{D} = C_P \mathbf{e}_P + C_S \mathbf{e}_S + C_Q \mathbf{e}_Q + \sum_{j=5, \dots, N+1} C_j \mathbf{e}_j. \tag{13}$$

In this case, the scalar product of wave vectors turns into the conventional dot product of Euclidean vectors: $\langle Br||D\rangle = (\mathbf{R}\mathbf{D})$. Since the subspace of dark states is orthogonal to the bright state at time t , all the dark state geometrical counterparts (d-vectors) (13) must lie in a plane $\Pi_D(t)$ tangent to the unit sphere at the point $\mathbf{e}_r(t)$.

3.2 Parallel transport of dark vectors

In what follows, we consider adiabatic processes meeting the Massey criterion (1) that prevents population transfer between dark and bright states. Thus, the state vector $\psi(t)$ (2), if initially prepared as a dark state,

must always remain in the dark subspace. In accordance with [18, 19], the temporal dynamics of dark states due to the nonadiabatic coupling operator is reduced to a group U_{N-1} of unitary transformations in the manifold Λ_D . In geometrical terms, these dynamics equal the parallel transport of the tangent d-vectors along the Rabi path $\mathfrak{S}_1 = \widehat{\Xi}_{R \rightarrow 1} \mathfrak{S}_R$.

As applied to tripod systems, Fig. 3 illustrates the Riemannian parallel transport [14] of the initial tangent d-vector \mathbf{D}_0 along the circular path Υ_λ lying on the two-dimensional Bloch sphere. The circle Υ_λ with latitude λ is situated in a plane parallel to the coordinate plane (Q, S) . The momentary tangent plane $\Pi_D(\varphi)$ is spanned by the two natural basis vectors $\mathbf{e}_\varphi(\varphi), \mathbf{e}_\theta(\varphi)$, related to the azimuthal φ and polar θ coordinate angles, respectively. The angle φ plays the role of a time variable t . An explicit relationship between t and φ is provided in the next section.

Our aim is to obtain an explicit analytical expression for the transported d-vector $\mathbf{D}(\varphi)$, provided its initial value \mathbf{D}_0 at the angle $\varphi = 0$. Three components $C_{Q,S,P}(\varphi)$ of $\mathbf{D}(\varphi)$ correspond to the state vector $\psi(\varphi)$

$$\begin{aligned} \psi(\varphi) &= C_Q |4\rangle + C_S |3\rangle + C_P |1\rangle \Leftrightarrow \mathbf{D}(\varphi) \\ &= C_Q \mathbf{e}_Q + C_S \mathbf{e}_S + C_P \mathbf{e}_P, \end{aligned} \tag{14}$$

which should be the solution of the Schrödinger equation (2). In the next section, we compare the dynamics of the wave vector ψ obtained using the geometrical approach (see Eqs. (19)–(21)) with the results of numerical simulations of the quantum equation (2).

In the case of a tripod configuration with two-dimensional tangent plane, a parallel transport of the d-vector \mathbf{D} along the circle Υ_λ results in rotation of $\mathbf{D}(\varphi)$ by angle β_φ in the tangent plane $\Pi_D(\varphi)$ (see Fig. 3), i.e.,

$$\mathbf{D}(\varphi) = \cos \beta_\varphi \cdot \mathbf{e}_\theta(\varphi) + \sin \beta_\varphi \cdot \mathbf{e}_\varphi(\varphi) \tag{15}$$

Because of the obvious rotation symmetry of the problem under study, the corresponding accumulated angle β_φ , shown in Fig. 3, has a linear dependence on the “parametric time” φ :

$$\beta_\varphi = \varsigma \cdot \varphi; \quad \varsigma = \sin \lambda \tag{16}$$

The value of the coefficient ς can be found from the well-known Riemann theorem [13, 14], which states that after a full revolution along the circle Υ_λ the rotation angle $\beta_{2\pi}$ is equal to the area of the surface subtended on the Bloch sphere by the circle: $\beta_{2\pi} = 2\pi \sin \lambda$.

In accordance with Fig. 3, the basis vectors in plane $\Pi_D(\varphi)$ read

$$\mathbf{e}_\varphi(\varphi) = -\sin \varphi \cdot \mathbf{e}_Q + \cos \varphi \cdot \mathbf{e}_S; \tag{17}$$

$$\mathbf{e}_\theta(\varphi) = \cos \lambda \cdot \mathbf{e}_P - \sin \lambda \cdot (\cos \varphi \cdot \mathbf{e}_Q + \sin \varphi \cdot \mathbf{e}_S) \tag{18}$$

A combination of Eqs. (14)–(18) yields the following evolution of the dark state $\psi(\varphi)$ (14) upon changing

the parametric time φ :

$$C_4 = C_Q = -\cos \beta_\varphi \sin \lambda \cos \varphi - \sin \beta_\varphi \sin \varphi \tag{19}$$

$$C_3 = C_S = -\cos \beta_\varphi \sin \lambda \sin \varphi + \sin \beta_\varphi \cos \varphi \tag{20}$$

$$C_1 = C_P = \cos \beta_\varphi \cos \lambda \tag{21}$$

At the same time, the vector $\mathbf{e}_r(t)$ (12)

$$\mathbf{e}_r(\varphi) = \cos \lambda \cos \varphi \cdot \mathbf{e}_Q + \cos \lambda \sin \varphi \cdot \mathbf{e}_S + \sin \lambda \cdot \mathbf{e}_P \tag{22}$$

determines the required parametric time dependence of periodic laser pulses Ω_j :

$$\frac{\Omega_Q}{\Omega_{\text{eff}}} = \cos \lambda \cos \varphi; \quad \frac{\Omega_S}{\Omega_{\text{eff}}} = \cos \lambda \sin \varphi; \quad \frac{\Omega_P}{\Omega_{\text{eff}}} = \sin \lambda. \tag{23}$$

Here, in accordance with Eqs. (7), (8) and Fig. 2, the parameter Ω_{eff} is the effective Rabi frequency.

4 Numerical experiment for tripod system and discussion

Under a real experimental situation, one should deal with its specific timescale. In the analytical representations of the Rabi frequencies (23) and the corresponding geometric evolution (19)–(21) of the dark state vector, it is convenient to set a linear relationship between the dimensionless time parameter φ and the actual time t , namely

$$\varphi = 2\pi t/T; \quad \xi = \frac{1}{2} T \Omega_{\text{eff}}, \tag{24}$$

where T is the period of laser pulses, while ξ (with reference to definition (1), Eq. (11), and Fig. 1) is the Massey parameter. In the following subsections, we consider the single-photon detuning Δ to be zero.

4.1 Collation of numerical simulation with the geometric approach

In this subsection, we compare the geometrical description (19)–(21) of the state vector ψ (14) evolution in a tripod system with explicit numerical solutions of the Schrödinger equation (2) for several typical examples of trigonometrical control laser pulses (23). It will be shown, in particular, how perfect adiabaticity improves the fidelity of our geometric approach as the Massey parameter (24) increases. Noteworthy, our model problems are parameterized with although geometrical, but somewhat formal parameter λ . The rotation angle $\beta_{2\pi} = 2\pi \cdot \sin \lambda$ (16) of the dark state vector \mathbf{D}_φ during a full cycle of laser pulses (see Fig. 3) has a more physical interpretation.

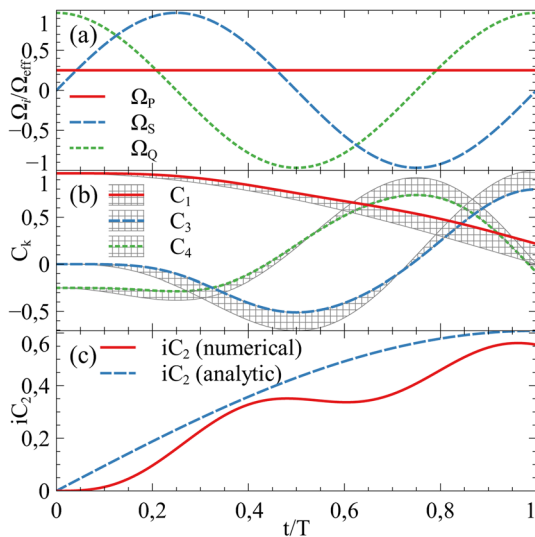


Fig. 4 Sequence of laser Rabi frequencies $\Omega_{P,S,Q}(t)$ (frame **a**) and the corresponding numerical solutions (bold lines) of Schrödinger equation (2) for probability amplitudes $C_{1,3,4}$ (frame **b**) for the ground subspace Λ_g and iC_2 (frame **c**) for the excited state $|2\rangle$. The case of $\beta_{2\pi} = \pi/2$ and the Massey parameter (24) $\xi=10$ is considered. Highlighted areas in frame (b) represent deviation from the geometrically obtained analytical solutions (19–21), and the dashed line in frame (c) represents the analytical solution (28)

The data on probability amplitudes $C_{1,3,4}$ and iC_2 shown in Figs. 4, 5, 6 and marked with bold lines were obtained numerically (solutions to the Schrödinger equation (2)). The corresponding geometric solutions are shown with thin or dashed lines. Where distinguishable, the deviations of numerical data from the analytical results are highlighted with rectangular mesh of thin lines (see frame (b) in Fig. 4).

4.2 Discussion

For the model N-pod system, we have identified a mapping of the singular bright (Br) and $(N - 1)$ -fold degenerate dark dressed states to the Euclidean parameter space of N Rabi frequencies Ω_j . The Br state is mapped onto the unit sphere (Bloch sphere) of the parametric space, while the geometric counterparts of the dark states lie on the $(N - 1)$ -dimensional plane tangent to the Bloch sphere at the point counterpart of the Br state (see Fig. 3). A complete cycle of pulsed laser excitations on the system results in the Br state drawing a closed loop \mathfrak{S}_1 (circle Υ_λ in Fig. 3) on the Bloch sphere. The quantum dynamics of the subsystem of dark states translates into the procedure of Riemannian parallel transport of tangent planes along the \mathfrak{S}_1 loop.

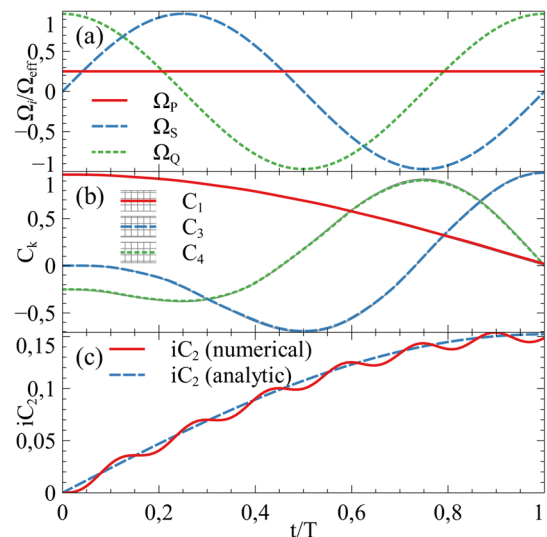


Fig. 5 Same situation as in Fig. 4 for $\beta_{2\pi} = \pi/2$ but with increased Massey parameter value $\xi=40$. The larger ξ -value corresponds to improved adiabaticity, and the numerical solutions very closely follow the geometrical solutions (19–21). It is shown the sequence of laser Rabi frequencies $\Omega_{P,S,Q}(t)$ (frame **a**) and the corresponding geometrical (dashed lines) or numerical (bold lines) solutions of Schrödinger equation (2) for probability amplitudes $C_{1,3,4}$ (frame **b**) related to the ground subspace Λ_g , along with iC_2 one (frame **c**) for the excited state $|2\rangle$

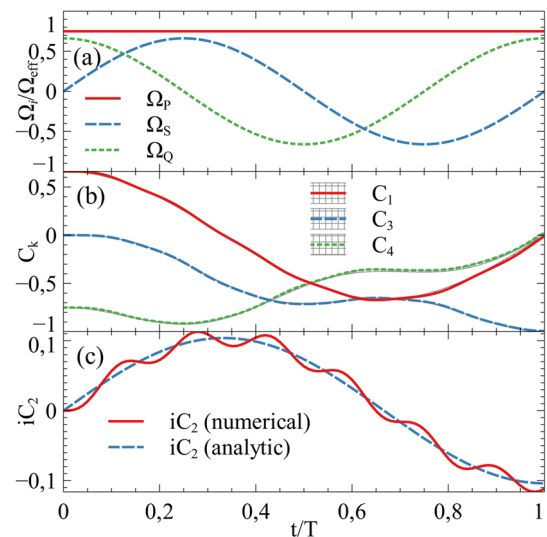


Fig. 6 Same situation as in Fig. 4 but with $\beta_{2\pi} = 3\pi/2$ and increased Massey parameter value $\xi=40$. It is shown the sequence of laser Rabi frequencies $\Omega_{P,S,Q}(t)$ (frame **a**) and the corresponding geometrical (dashed lines) or numerical (bold lines) solutions of Schrödinger equation (2) for probability amplitudes $C_{1,3,4}$ (frame **b**) related to the ground subspace Λ_g , along with iC_2 one (frame **c**) for the excited state $|2\rangle$

Our numerical data obtained for the case of tripod system and presented in Fig. 4 show some discrepancy between the numerical and analytical results in the case of a relatively small value of the Massey parameter $\xi = 10$. This discrepancy is caused by the nonadiabatic coupling between dark and bright states and the consequential excitation of the upper state $|2\rangle$, evident from the Rabi oscillations in iC_2 (see panel (c) in Figs. 4, 5, 6). The nonadiabatic effects are reduced by increasing the value of Massey parameter, blocking the population outflow from the dark subspace into the bright states. This in turn improves the accuracy of the geometric results, which is clearly shown in Figs. 5 and 6, where the Massey parameter value is set to $\xi = 40$. One of the advantages of our analytical description (19)–(21) for the state vector (14) is connected with the possibility of giving accurate enough assessment for the nonadiabatic effects in the limit of large Massey parameter ξ , when the above-mentioned outflow does not have a noticeable effect on the dynamics of the dark state vector (14).

We start by finding the geometrical counterpart for the matrix element

$$\begin{aligned} M_{DB} &\equiv i\hbar \langle \psi(\varphi) | \frac{\partial}{\partial t} | Br(\varphi) \rangle \\ &= i\hbar \frac{d\varphi}{dt} \langle \psi(\varphi) | \frac{\partial}{\partial \varphi} | Br(\varphi) \rangle \end{aligned} \quad (25)$$

of the nonadiabatic coupling operator [5, 18] between the dark $|\psi\rangle$ and bright states $|Br\rangle$. As it follows from the notation in Fig. 2, upon parallel transport along the circle Υ_λ , one has

$$\frac{\partial}{\partial \varphi} | Br(\varphi) \rangle = \frac{\partial}{\partial \varphi} e_r(\varphi) = r_\lambda e_\varphi; \quad (\mathbf{D}_\varphi e_\varphi) = \sin \beta_\varphi; \quad (26)$$

therefore, the matrix element can be expressed as

$$M_{DB} = i\hbar r_\lambda \frac{2\pi}{T} \sin \beta_\varphi; \quad r_\lambda = \cos \lambda. \quad (27)$$

Here β_φ is the current rotation angle (16), r_λ is the radius of the circle Υ_λ , and the dependence $\varphi(t)$ is given by Eq. (24).

Importantly, in the first adiabatic approximation, the manifold of dark states shown in Fig. 2b can be replaced by a single state vector $\psi(t)$. The corresponding linkage diagram becomes identical to the simple Λ -scheme with $|Br\rangle$ as an intermediate state coupled to $|2\rangle$ and $\psi(t)$ levels by Ω_{eff} and $2M_{DB}/\hbar$ Rabi frequencies consequently. The Massey criterion of adiabaticity $\xi \gg 1$ allows to apply the procedure of adiabatic elimination [11, 20] for that Λ -scheme resulting in the following dynamics of probability amplitudes for the strongly coupled pair:

$$C_2(\varphi) \cong -\frac{2M_{DB}}{\hbar\Omega_{\text{eff}}} = -i\frac{2\pi}{\xi} \cos \lambda \cdot \sin(\sin \lambda \cdot \varphi);$$

$$C_{Br} \cong 0. \quad (28)$$

In other words, in the limit of strong adiabaticity, the amplitude C_2 instantly follows a relatively slow change in the corresponding nonadiabaticity matrix element M_{DB} (27) and turns out to be weakly subject to fast Rabi oscillations of frequency Ω_{eff} between amplitudes of bright $|Br\rangle$ and excited $|2\rangle$ states (see Fig. 2b). Frames (c) in Figs. 5 and 6 illustrate well the fidelity of our theoretical findings for iC_2 .

5 Conclusion

In the physics of inelastic collision processes, the Landau–Zener theory is the main theoretical tool for assessing the probabilities of various localized transitions between quantum states. Significant delocalization of the quantum transitions due to, for example, the energy degeneration of the levels in question leads to a noticeable complication of the mathematical apparatus necessary for the situation analysis. This article proposes a novel purely geometric approach to studying nonadiabatic dynamics in multilevel systems based on the Riemannian concept of parallel transport of tangent vectors on curvilinear surfaces.

Adequacy of the geometric approach is demonstrated on a model N-pod atomic system (see Fig. 2a), which, regardless of the number of control lasers, has a universal structure of bright and dark adiabatic states (see Fig. 2b). The N laser Rabi frequencies Ω_j play the role of control parameters. Their instantaneous values determine the composition of the adiabatic states, and changing the Rabi frequencies triggers nonadiabatic transitions, which is the primary mechanism driving dynamics of the $(N - 1)$ -fold degenerate dark manifold. We have demonstrated a natural mapping of quantum wave vectors to the N -dimensional Euclidean parameter space $\{\Omega_j\}$, where quantum dynamics of the dark subspace translates into Riemannian parallel transport of a tangent plane along a path \mathfrak{S}_1 on the surface of the unit sphere (Bloch sphere). Comparison between quantum (solutions of the Schrödinger equation) and geometric (parallel transport) calculations of the state vector $\psi(t)$ dynamics in a tripod ($N=3$) system has revealed the absolute identity of the solutions, provided the situation meets the adiabaticity criterion of large Massey parameter values ξ (1).

In addition to academic interest, the N-pod systems have attracted attention as promising physical objects for quantum information processing [4, 12] and for solving other modern physical problems. Tripod systems ($N = 3$) are already being widely used in quantum memory formation [21], quantum computing with one qubit [4], quantum simulations of gauge potentials [22, 23], etc. In [24], the geometric approach described here was used to construct highly efficient rotation quantum gates based on a tripod system. In higher-dimensional ($N > 3$) systems, it enables research on multidimensional generalizations of the qubit (so-called

qudit), which was demonstrated in [12] for example of constructing generalized quantum Householder reflections of dimension $(N-1)$. We believe that the approach of merging the adiabatic formalism with conventional group theory methods will promote development of novel, efficient algorithms for emerging quantum technologies.

Acknowledgements This work was supported by Latvian Council of Science Grant No. LZP-2019/1-0280.

Author contributions

All the authors were involved in the preparation of the manuscript. All the authors have read and approved the final manuscript.

Data Availability Statement This manuscript has associated data in a data repository. [Authors' comment: All data generated during this study are contained in this published article.]

References

1. E.E. Nikitin, S.Y. Umanskii, *Theory of Slow Atomic Collisions*. Springer, Berlin, Heidelberg (1984). <https://doi.org/10.1007/978-3-642-82045-8>
2. N.N. Bezuglov, R. Garcia-Fernandez, A. Ekers, K. Miculis, L.P. Yatsenko, K. Bergmann, Consequences of optical pumping and interference for excitation spectra in a coherently driven molecular ladder system. *Phys. Rev. A* (2008). <https://doi.org/10.1103/physreva.78.053804>
3. N.V. Vitanov, A.A. Rangelov, B.W. Shore, K. Bergmann, Stimulated Raman adiabatic passage in physics, chemistry, and beyond. *Rev. Mod. Phys.* (2017). <https://doi.org/10.1103/revmodphys.89.015006>
4. K. Bergmann, H.-C. Nägerl, C. Panda, G. Gabrielse, E. Miloglyadov, M. Quack, G. Seyfang, G. Wichmann, S. Ospelkaus, A. Kuhn, S. Longhi, A. Szameit, P. Pirro, B. Hillebrands, X.-F. Zhu, J. Zhu, M. Drewsen, W.K. Hensinger, S. Weidt, T. Halfmann, H.-L. Wang, G.S. Paroanu, N.V. Vitanov, J. Mompart, T. Busch, T.J. Barnum, D.D. Grimes, R.W. Field, M.G. Raizen, E. Narevicius, M. Auzinsh, D. Budker, A. Pálffy, C.H. Keitel, Roadmap on stirap applications. *J. Phys. B At. Mol. Opt. Phys.* **52**(20), 202001 (2019). <https://doi.org/10.1088/1361-6455/ab3995>
5. L.I. Schiff, *Quantum Mechanics*, 3rd edn. (McGraw-Hill, New York, 1968)
6. B.W. Shore, Picturing stimulated Raman adiabatic passage: a stirap tutorial. *Adv. Opt. Photon.* **9**(3), 563–719 (2017). <https://doi.org/10.1364/AOP.9.000563>
7. L.D. Landau, E.M. Lifshitz, *Quantum Mechanics: Non-relativistic Theory. Course of Theoretical Physics* (Butterworth-Heinemann, Oxford, 1981)
8. A. Dykhne, Quantum transitions in the adiabatic approximation. *Sov. Phys. JETP* **11**, 411 (1960)
9. J.P. Davis, P. Pechukas, Nonadiabatic transitions induced by a time-dependent Hamiltonian in the semiclassical/adiabatic limit: the two-state case. *J. Chem. Phys.* **64**(8), 3129–3137 (1976). <https://doi.org/10.1063/1.432648>
10. K. Blum, *Density Matrix Theory and Applications*, 3rd edn. Springer Series on Atomic, Optical, and Plasma Physics. Springer, Heidelberg (2012). doi:<https://doi.org/10.1007/978-3-642-20561-3>
11. L. Allen, J.H. Eberly, *Optical Resonance and Two-level Atoms. Dover Books on Physics and Chemistry* (Dover, New York, 1987)
12. B. Rousseaux, S. Guérin, N.V. Vitanov, Arbitrary qudit gates by adiabatic passage. *Phys. Rev. A* **87**, 032328 (2013). <https://doi.org/10.1103/PhysRevA.87.032328>
13. E. Kreyszig, *Differential Geometry. Differential Geometry* (Dover Publications, New York, 1991)
14. V.I. Arnold, *Mathematical Methods of Classical Mechanics*. Springer, New York (1978). <https://doi.org/10.1007/978-1-4757-1693-1>
15. A. Cinins, M. Bruvelis, M.S. Dimitrijević, V.A. Srećković, D.K. Efimov, K. Miculis, N.N. Bezuglov, A. Ekers, Expressions of “fast” and “slow” chameleon dressed states in Autler–Townes spectra of alkali-metal atoms. *Astronomische Nachrichten* **343**(1–2), 210081 (2022). <https://doi.org/10.1002/asna.20210081>
16. J.R. Morris, B.W. Shore, Reduction of degenerate two-level excitation to independent two-state systems. *Phys. Rev. A* **27**, 906–912 (1983)
17. T. Kirova, A. Cinins, D.K. Efimov, M. Bruvelis, K. Miculis, N.N. Bezuglov, M. Auzinsh, I.I. Ryabtsev, A. Ekers, Hyperfine interaction in the Autler–Townes effect: the formation of bright, dark, and chameleon states. *Phys. Rev. A* **96**, 043421 (2017). <https://doi.org/10.1103/PhysRevA.96.043421>
18. F. Wilczek, A. Zee, Appearance of gauge structure in simple dynamical systems. *Phys. Rev. Lett.* **52**, 2111–2114 (1984). <https://doi.org/10.1103/PhysRevLett.52.2111>
19. L.D. Faddeev, A.A. Slavnov, *Gauge Fields. Introduction to Quantum Theory* (The Benjamin/Cummings Publishing Company Inc, Reading, 1980)
20. D.K. Efimov, M. Bruvelis, N.N. Bezuglov, M.S. Dimitrijević, A.N. Klyucharev, V.A. Srećković, Y.N. Gnedin, F. Fuso, Nonlinear spectroscopy of alkali atoms in cold medium of astrophysical relevance. *Atoms* (2017). <https://doi.org/10.3390/atoms5040050>
21. A.S. Losev, T.Y. Golubeva, A.D. Manukhova, Y.M. Golubev, Two-photon bunching inside a quantum memory cell. *Phys. Rev. A* (2020). <https://doi.org/10.1103/physreva.102.042603>
22. J. Ruseckas, G. Juzeliūnas, P. Öhberg, M. Fleischhauer, Non-abelian gauge potentials for ultracold atoms with degenerate dark states. *Phys. Rev. Lett.* **95**, 010404 (2005). <https://doi.org/10.1103/PhysRevLett.95.010404>

23. J. Dalibard, F. Gerbier, G. Juzeliūnas, P. Öhberg, Colloquium: artificial gauge potentials for neutral atoms. *Rev. Mod. Phys.* **83**, 1523–1543 (2011). <https://doi.org/10.1103/RevModPhys.83.1523>
24. A. Cinins, M. Bruvelis, N.N. Bezuglov, Study of the adiabatic passage in tripod atomic systems in terms of the Riemannian geometry of the Bloch sphere. *J. Phys. B At. Mol. Opt. Phys.* **55**(23), 234003 (2022). <https://doi.org/10.1088/1361-6455/ac9a90>

Springer Nature or its licensor (e.g. a society or other partner) holds exclusive rights to this article under a publishing agreement with the author(s) or other rightsholder(s); author self-archiving of the accepted manuscript version of this article is solely governed by the terms of such publishing agreement and applicable law.